



Original Article

High-temperature interaction of oxygen-preloaded Zr1Nb alloy with nitrogen

Martin Steinbrück*, Stefen Prestel, Uta Gerhards

Karlsruhe Institute of Technology, Karlsruhe, Germany

ARTICLE INFO

Article history:

Received 26 October 2017

Received in revised form

5 December 2017

Accepted 11 December 2017

Available online 15 February 2018

Keywords:

Air Ingress

Kinetics

Nitrogen

Zirconium Alloy

ABSTRACT

Potential air ingress scenarios during accidents in nuclear reactors or spent fuel pools have raised the question of the influence of air, especially of nitrogen, on the oxidation of zirconium alloys, which are used as fuel cladding tubes and other structure materials. In this context, the reaction of zirconium with nitrogen-containing atmospheres and the formation of zirconium nitride play an important role in understanding the oxidation mechanism. This article presents the results of analysis of the interaction of the oxygen-preloaded niobium-bearing alloy M5[®] with nitrogen over a wide range of temperatures (800–1400°C) and oxygen contents in the metal alloy (1–7 wt.%). A strongly increasing nitriding rate with rising oxygen content in the metal was found. The highest reaction rates were measured for the saturated α -Zr(O), as it exists at the metal–oxide interface, at 1300°C. The temperature maximum of the reaction rate was approximately 100 K higher than for Zircaloy-4, already investigated in a previous study [1]. The article presents results of thermogravimetric experiments as well as posttest examinations by optical microscopy, scanning electron microscopy (SEM), and microprobe elemental analyses. Furthermore, a comparison with results obtained with Zircaloy-4 will be made.

© 2018 Korean Nuclear Society, Published by Elsevier Korea LLC. This is an open access article under the CC BY-NC-ND license (<http://creativecommons.org/licenses/by-nc-nd/4.0/>).

1. Introduction

Zirconium alloys are used worldwide in the nuclear industry for fuel claddings and other structural materials because of their good mechanical properties and corrosion resistance at operational conditions as well as because of their low cross section for thermal neutrons. However, during loss-of-coolant accidents as well as severe nuclear accidents, the high-temperature oxidation of zirconium by water steam causes serious degradation of the mechanical properties of cladding tubes, resulting in the loss of barrier effect against the release of fission products, as well as in the production of hydrogen and chemical heat. The hydrogen source term due to the zirconium-steam reaction carries the risk of hydrogen detonation, as was seen during the Fukushima Daiichi accidents. The chemical heat produced by the oxidation reaction may exceed the nuclear decay heat at high temperatures, thus becoming a driving force for thermal excursions of the reactor core [2].

Numerous studies on the oxidation of zirconium alloys in water steam have been conducted over a wide range of temperatures and conditions during the last decades, mainly triggered by the TMI-2

accident 1979 in the United States [3,4]. Air ingress scenarios in reactors have also been discussed for a long time; see for example the study by Powers et al. [5]. After the Fukushima accidents, air ingress accident scenarios for spent fuel pools came into focus for international research [6].

It is known from many experimental studies that the oxidation of zirconium alloys by steam or oxygen is strongly affected by the presence of nitrogen [7] [8–12]. Especially in the temperature range between 800°C and 1200°C, the reaction kinetics are strongly increased by nitrogen, resulting in more severe degradation of the cladding and higher hydrogen source terms (if steam is available) compared to oxidation in pure steam and oxygen atmosphere. The understanding of the mechanism of nitrogen attack is that zirconium nitride, ZrN, is temporarily formed and subsequently reoxidized; this is connected with serious volume mismatches because of the different densities of the involved phases, and with this the formation of non-protective oxide scales. Furthermore, it is known that, on the one hand, the reaction of zirconium with nitrogen is very slow due to the formation of a thin protective nitride scale and low diffusion coefficients of nitrogen in Zr [13], but, on the other hand, much ZrN is formed during the reaction of oxygen-stabilized zirconium with nitrogen [9]. Conditions favorable for the formation of ZrN are present locally at the metal–oxide interface after consumption of oxygen when nitrogen is in contact with the oxygen-

* Corresponding author.

E-mail address: martin.steinbrueck@kit.edu (M. Steinbrück).

stabilized α -Zr(O) phase. The results of a systematic study of the interaction between oxygen-stabilized α -Zr(O) prepared from the tin-bearing alloy Zircaloy-4 with nitrogen has been published recently; this study showed a strong influence of the oxygen content in the metal, and of the temperature, on the reaction kinetics with nitrogen [1]. This article presents results of complementary experiments with the niobium-bearing alloy M5[®], produced by AREVA (France).

2. Experimental details

2.1. Test setup

All experiments presented in this article were conducted in a commercial thermal balance (NETZSCH STA-409) with a vertical tube furnace and balance below the furnace, coupled via a capillary with a quadrupole mass spectrometer (NETZSCH Aeolos); details are described in the study by Steinbrück et al. [14]. The gases (Ar, O₂, N₂) were supplied via Bronkhorst[®] flow controllers at the lower part of the vertical tube furnace. Argon flowed through the balance containment into the furnace; the reaction gases were directly injected into the reaction tube to prevent contamination of the balance and to ensure a well-defined gas mixture in the furnace. All gases used were highly pure, with less than one and 10 ppm impurities, respectively.

2.2. Specimens

M5[®] is an advanced cladding alloy produced by AREVA for pressurized water reactors; it has approximately 1 wt.% niobium and 0.13 wt.% oxygen as main alloying components. Tube segments 2 cm long (10.75 mm outer diameter and 0.725 mm wall thickness) were cut from longer tubes, deburred and ground at both ends, and cleaned in an ultrasonic bath of acetone. The samples were positioned vertically on an yttrium oxide plate in the furnace of the thermal balance. Tubes were open at the ends; consequently, reactions of the gases with the inner and outer surface of the tube segments were possible, but with different thermohydraulic boundary conditions due to the bottom-up gas flow.

2.3. Test procedure

The objective of this study was the investigation of the α -Zr(O) reaction with nitrogen as a function of temperature and oxygen content of the metal in the whole phase region of α -Zr(O). Reasonable reaction rates were achieved at temperatures from 800°C; the upper temperature limit was 1400°C. The test matrix is shown by red dots in the Zr-O phase diagram [15] in Fig. 1.

Argon was used as carrier gas and reference gas for mass spectroscopy in all tests. This will be not explicitly mentioned in the rest of the article. The use of argon may have some influence on gas diffusion, especially in pores and cracks. Investigation of such an effect was not within the scope of the report. The argon flow rate during all tests was 3 l/h. The flow rate of oxygen during preoxidation (PO) was 1–3 l/h; that for nitrogen during the nitriding phase was 10 l/h.

As shown in Fig. 2, the specimens were subjected to (1) slow and manually controlled PO in oxygen at 1200°C until the desired mass gain was obtained, leading to a circumferentially and axially homogeneous oxygen uptake, (2) 3 hour of homogenization in argon at 1400°C, and (3) 1 hour of reaction at the predefined temperature (800–1400°C) in nitrogen. The use of oxygen (instead of water steam, which for nuclear accidents would be more prototypical) allowed in-situ preparation and investigation within one thermogravimetric (TG) experiment. In any case, hydrogen, possibly taken up during PO in steam, would have been completely released during the homogenization phase according to Sieverts' law [16]. Fig. 3 shows two micrographs with through-wall cross section taken after the preoxidation and after the homogenization phase, proving the dissolution of the oxide scale during 3 hour at 1400°C in inert atmosphere. Owing to the short duration of the oxidation phase and the low oxygen mass flow rate, the tube segment was only oxidized externally at the points to which oxygen had direct access.

2.4. Posttest examinations

Macro photos were taken of all specimens after the tests. Then, the specimens were embedded in epoxy resin, cut, ground, and polished for metallographic examination by optical microscopy. The local composition of selected samples, especially with regard to

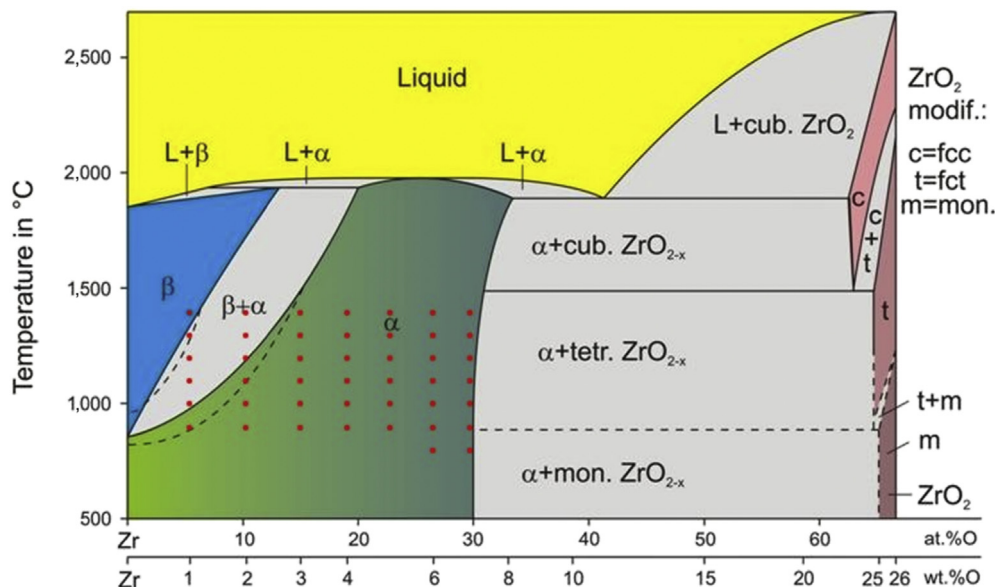


Fig. 1. Phase diagram Zr-O [15] with test matrix shown by red dots.

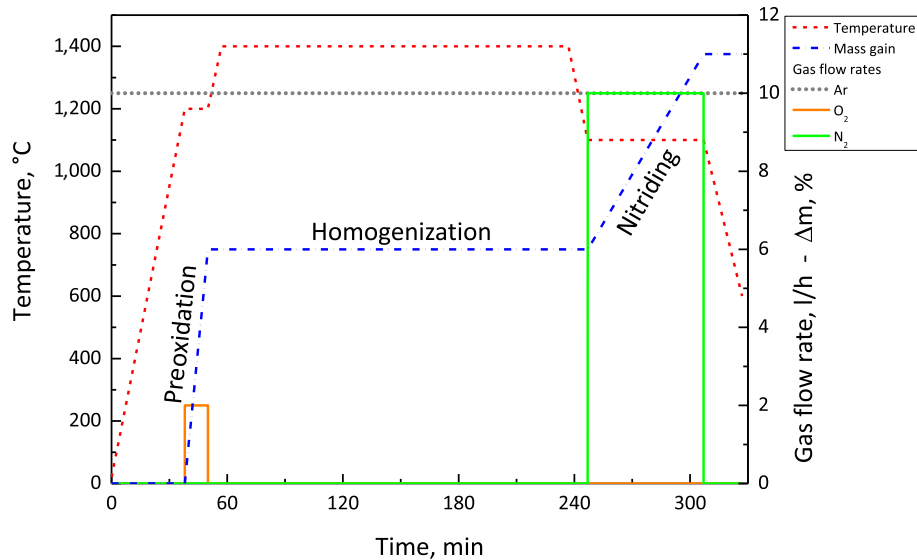


Fig. 2. Schematic test conduct with temperature history, gas flow rates, and mass gain signal. Here: (i) preoxidation in oxygen resulting in a mass gain of 6 wt.%, (ii) 3 h homogenization at 1400°C, and (iii) 1 h nitriding at 1100°C.

oxygen and nitrogen, was analyzed by a JEOL JXA-8530F Field Emission Electron Probe Microanalyzer with 5 kV acceleration voltage and 50 nA probe current; for element mapping, values of 10 kV and 50 nA were used. Under these conditions, the dimensions of the activation volume are smaller than 1 μm for both ZrN and ZrO_2 . To limit surface contamination of the samples, they were again polished and covered with an approximately 10 nm thick carbon layer directly before microprobe analysis.

3. Experimental results

3.1. Thermogravimetric results

The results of all thermogravimetric experiments are provided in Fig. 4. Only the nitriding phase is shown in these diagrams, i.e., the TG values were set to (0,0) with the initiation of the nitrogen flow. Generally, the nitriding kinetics is rather linear up to 1300°C, with exceptions discussed below. The mass gain of the samples strongly increases with oxygen content in the metal and, at least up to 1300°C, with temperature. Interestingly, most samples tested at 1400°C gained less mass than samples tested at 1300°C.

The initial slight, but fast, mass gain (best seen for the 800°C tests with highly magnified y-scale) is caused by residual oxygen in the gas inlet pipes that are used for active gases, oxygen, and nitrogen. The corresponding mass gain is less than 0.1 wt.% and can

be thus neglected. Starting from 1100°C, saturation is reached before the end of the test, especially for the samples with the highest degree of preoxidation. Saturation means (almost) complete oxidation or nitriding of the metal and leads theoretically, e.g., for $\text{PO} = 7$ wt.%, to a specific mass gain for complete nitriding of 288 g/m^2 . The initial mass gain caused by oxygen as well as the deviation from the linear curve due to saturation is not taken into account for the determination of the linear reaction rate coefficients. The gradual change of the slope of some TG curves, especially at higher temperatures, may be connected with the varying of active surfaces for the fast nitriding reaction; see results of posttest examinations given below.

3.2. Posttest appearance

Generally, the reaction was not always axially homogeneous; this should be taken into account for the analysis of the TG results. Usually, the nitriding started at one of the (or both) edges of the sample. The cladding segments were decorated by axial and circumferential cracks where zirconium nitride had formed during the annealing. The segments were very brittle and broke easily during handling. Fig. 5 provides an example of the posttest appearance of the sample with $\text{PO} = 7$ wt.% annealed in nitrogen at 1200°C. This sample was completely oxidized/nitrided as can be seen from the saturation in the TG curve and is confirmed by the

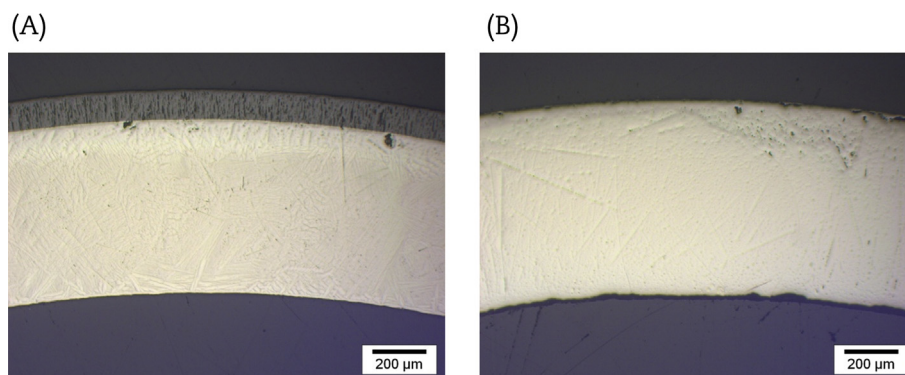


Fig. 3. Micrograph of M5® sample. (A) After 6 wt.% preoxidation. (B) After 6 wt.% preoxidation and subsequent homogenization according to the procedure shown in Fig. 2.

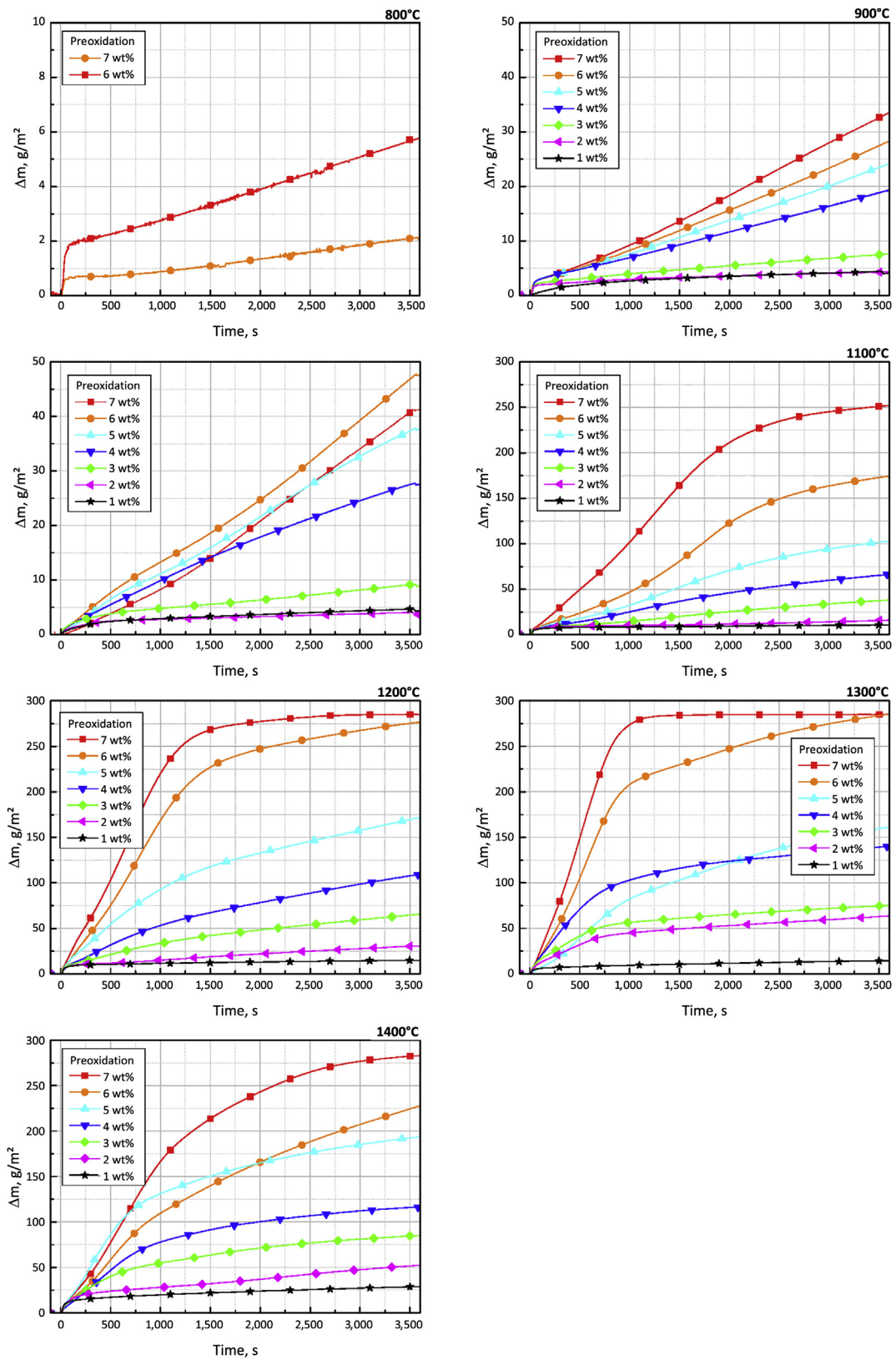


Fig. 4. Mass gain of preoxidized and homogenized M5[®] samples at temperatures from 800 to 1400°C in dependence on the oxygen concentration in the α -Zr(O) phase (please note the partly different scales of the y-axis).

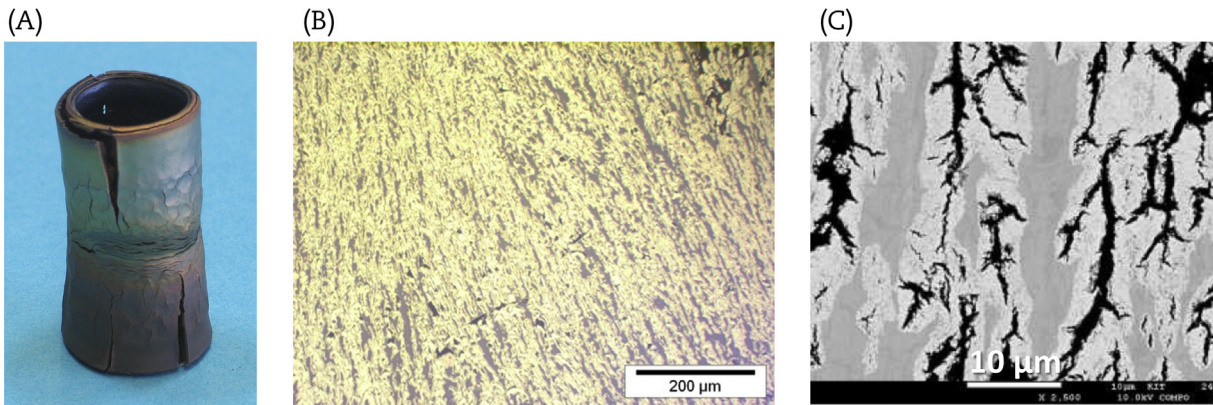


Fig. 5. Posttest appearance of the sample with 7 wt.% oxygen content and nitriding temperature of 1200°C. (A) Macrograph. (B) Optical micrograph. (C) SEM-back-scattered electrons (BSE) image.

optical micrograph image of the sample's cross section, which shows a two-phase mixture of gray zirconium oxide and golden-colored zirconium nitride. The SEM image with the largest magnification applied provides some more insight into the microstructure. The darker-gray oxide areas are dense, whereas cracks and pores run through the light-gray nitride phase.

Micrographs of the cross sections of all samples are compiled in Fig. 6. With rising content of preloaded oxygen and temperature, these micrographs show increasing formation of golden-colored zirconium nitride in the mixture with zirconium oxide. The microstructure of this two-phase mixture is relatively fine at lower temperatures (phase dimension < 5 µm at 900°C) and becomes coarser at higher temperatures (>50 µm at 1400°C). Some samples are completely converted to the ZrO_2/ZrN mixture after one hour

reaction time. Some other samples show a very local attack of nitrogen. For example, the wall of the specimen with PO = 6 wt.% annealed at 1200°C is completely consumed at one circumferential position and only slightly attacked at an adjacent one. Through-wall cracks are observed for many samples with and without strong nitride formation. The samples with only 1 wt.% preoxidation exhibit a surface zone that was affected by nitrogen. Most probably, a former β -Zr(O) or α - β -Zr(O) mixture was converted into pure α -Zr(O,N)-phase because of the reaction with nitrogen.

3.3. Microprobe elemental analyses

Microprobe analyses of all samples preloaded with 7 wt.% oxygen were performed to investigate the elemental composition and

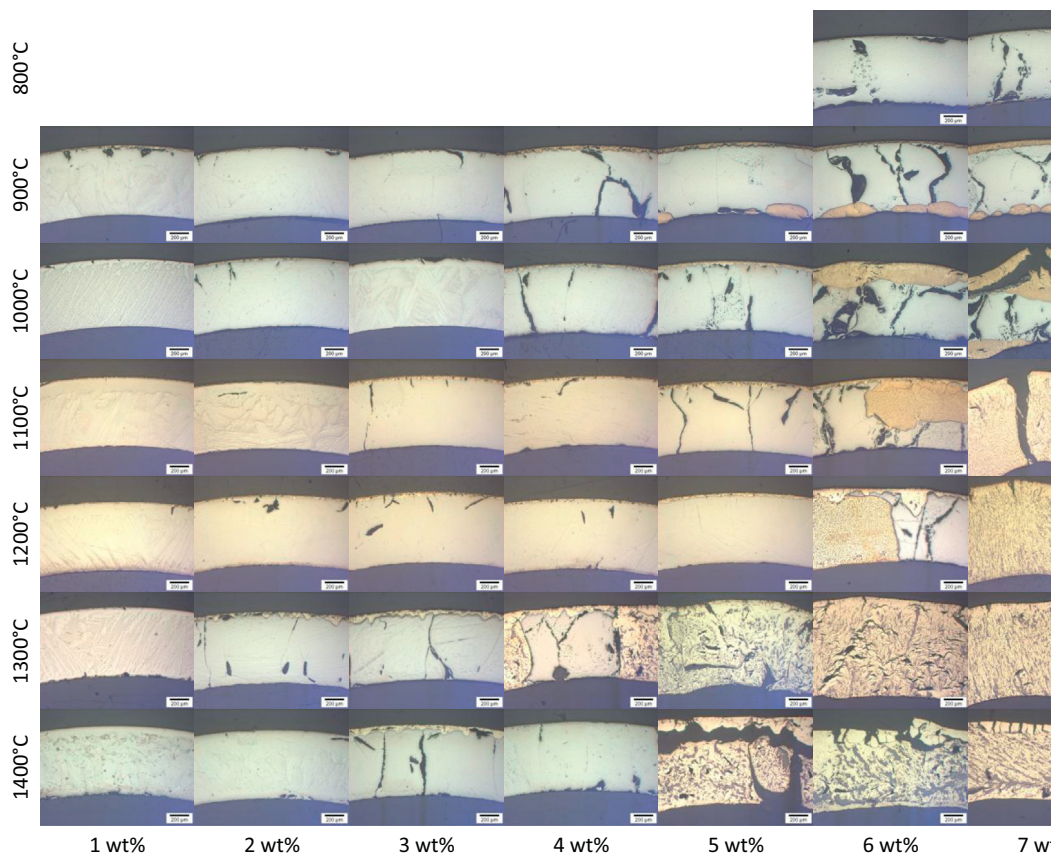


Fig. 6. Micrographs of through-wall cross sections of all samples in dependence on the degree of preoxidation and temperature.

the distribution of the involved phases, especially the diffusion of nitrogen into the α -Zr(O) phase before the formation of the oxide/nitride mixture and the mutual solubility of nitrogen in zirconia and oxygen in zirconium nitride. For these purposes, element mappings as well as quantitative radial line scans and point analyses including the elements Zr, O, and N were performed.

Fig. 7 presents an element map of one completely reacted sample. The morphology of the two-phase mixture of the sample nitrided at 1200°C clearly shows areas of oxide, nitride, and pores. The pores are located in the nitride phase, whereas the oxide phase is dense. There seems to be a gradient of oxygen concentration from the bulk to the edges of the oxide areas, indicated by the color change in the O mapping. Niobium is homogeneously distributed at least in the magnification chosen for these images.

More quantitative results were obtained by line scans. The diagrams in Fig. 8 show the concentrations of zirconium, oxygen, and nitrogen along a vertical line from the sample surface into the bulk. Furthermore, the degree of reaction (DoR) is indicated, which is defined as

$$DoR = 100 \left(\frac{C_O}{66.7} + \frac{C_N}{50} \right) \quad (1)$$

with C_O and C_N as concentrations in at.% of oxygen and nitrogen, respectively. DoR should be 100% if the analyzed sample area is completely oxidized and/or nitrided. The three examples given in Fig. 8 present samples with 7 wt.% oxygen only slightly nitrided at 800°C (A), with a locally formed ZrO₂/ZrN zone at 1000°C (B), and the completely reacted 1200°C sample (C). At 800°C, only a thin (<20 μm) nitride-containing scale has formed at the location of the line scan. Furthermore, nitrogen diffused into the α -Zr(O,N) phase up to a depth of approximately 120 μm. Obviously, oxygen-saturated α -Zr(O) is able to take up a certain amount of nitrogen before oxide and nitride are formed. The line scan in the Fig. 8B

shows the sharp transition from the oxide/nitride two-phase zone to an approximately 50 μm thick ZrO₂ layer and the oxygen-stabilized metal phase each within a few μm. Concentrations in the two-phase zones in the 1000°C sample and the completely reacted 1200°C sample naturally scatter strongly depending on whether oxide or nitride was analyzed. From Fig. 8C, it seems that there is always a limited oxygen concentration in the nitride, but at least at some positions no nitrogen is present in the oxide. The results of point analyses of various samples, where the nitride and oxide phase regions were larger than the typical activation volume of the electron beam for the microprobe analyses, were scattered between 0 and 10 at.% nitrogen in the oxide phase and between 4 and 12 at.% oxygen in the nitride phase. This confirms the values of the line scan in Fig. 8, taking into account that the depths of the phase regions and the interacting volume were not known; it cannot be ruled out that more than one phase was in the measured volume. The DoR (defined in Eq. (1)) is around 100% in the oxide/nitride mixture.

Generally, microprobe analyses have confirmed the intended oxygen contents (PO) as well as the homogeneity of the oxygen-loaded samples. The right parts of the line scans (with $C_N = 0$) of the samples annealed at 800°C and 1000°C show constant values of oxygen concentration of around 30 at.% (corresponding to 7 wt.%); this fits with the oxygen concentration of saturated α -Zr(O) according to the phase diagram, shown in Fig. 1.

Microprobe quantitative analysis of light elements may be impaired by surface oxidation; this effect cannot be completely excluded for the results presented here. The samples were freshly prepared before analysis to limit this effect. The very good accordance of the wavelength-dispersive X-ray spectroscopy (WDX) results with the target oxygen concentrations in the remaining α -Zr(O) phase should be an indication of reliable WDX results. The two other involved phases, ZrO₂ and ZrN, are less susceptible to such artifacts.

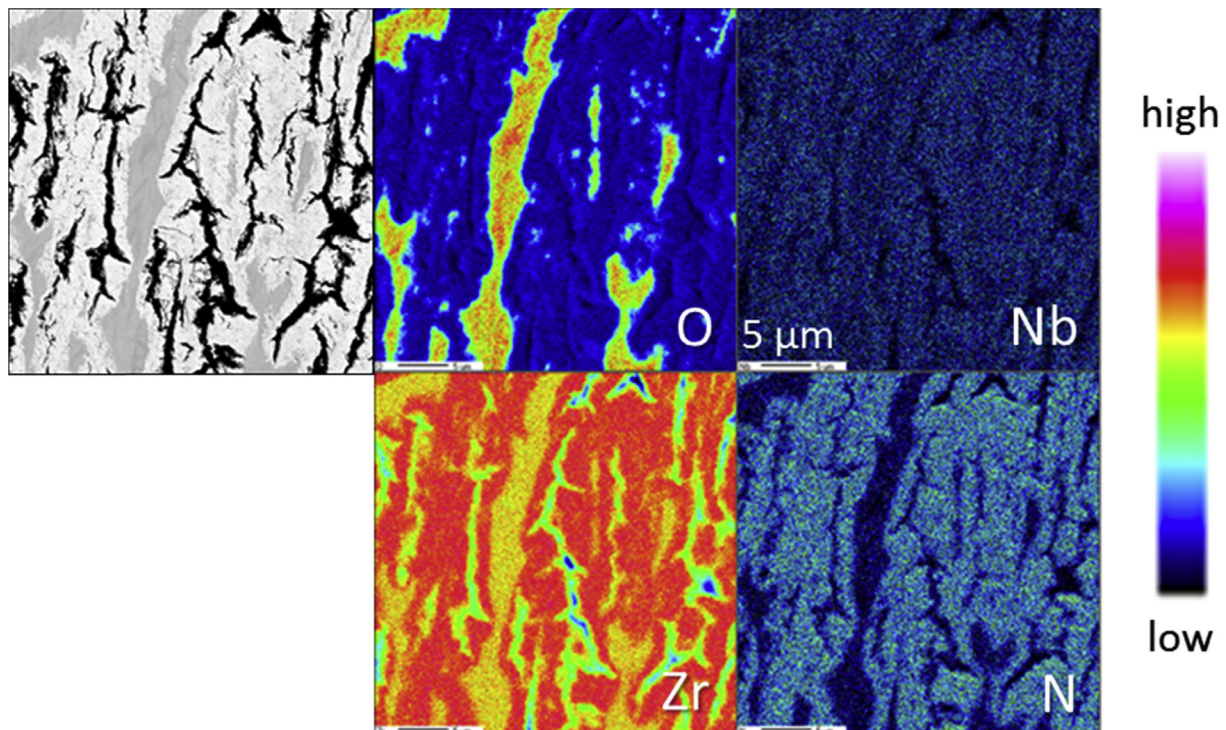


Fig. 7. Microprobe area scans of Zr, Nb, O, and N of the sample preloaded with 7 wt.% oxygen and annealed for 1 h in nitrogen at 1200°C. The SEM image of the scanned area is shown on the left side.

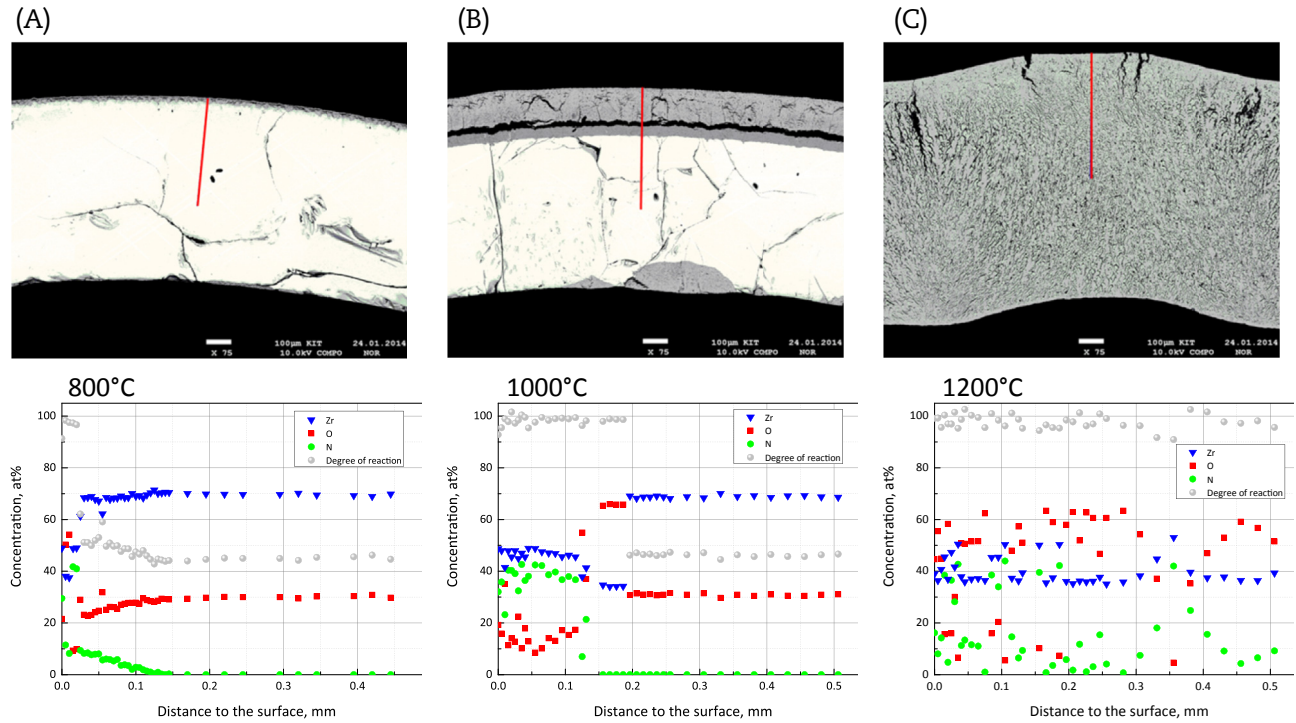


Fig. 8. Microprobe line scans of Zr, O, and N from the sample surfaces into the tube walls of samples preloaded with 7 wt.% oxygen and annealed for 1 h in nitrogen with corresponding BSE images at scan positions. (A) At 800°C; (B) At 1000°C; (C) At 1200°C. DoR, degree of reaction.

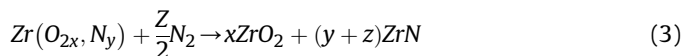
4. Discussion

The tests presented in the previous section confirmed the significant and mutual solubility of oxygen and nitrogen in zirconium. Based on TG and the posttest results of this study, the following reaction can be formulated:



for $2x < 0.42$ ($y = 0$) and $y < 0.30$ ($x = 0$), according to the known binary phase diagrams, which values correspond to DoR values of about 0.45 and 0.46, respectively. However, the α -Zr(O) phase seems to be able to dissolve more nitrogen than would be expected from the binary phase diagrams. Maximum values of $2x + y = 0.46$ (DoR = 0.61), according to Eq. (2), have been observed by microprobe analysis for specimens without formation of nitrides, e.g., at 800°C. No ternary phase diagram of the Zr-O-N system is available in the literature for comparison with the experimental data.

With a continuing reaction, the oxygen/nitrogen-stabilized α -phase converts to a ZrO₂/ZrN two-phase mixture when the solubility limit has passed, according to Eq. (3):



with $x + y + z = 1$ for the complete reaction.

The molar volumes of the involved phases are strongly different ($V_{m,\text{Zr}} = 14.0 \text{ cm}^3/\text{mol}$, $V_{m,\text{ZrN}} = 14.8 \text{ cm}^3/\text{mol}$, and $V_{m,\text{ZrO}_2(\text{monoclinic})} = 21.7 \text{ cm}^3/\text{mol}$). Thus, the reaction according to Eq. (3) is accompanied by the buildup of compressive and tensile stresses and the formation of cracks and pores, which are preferentially located along the ZrN grains with higher density.

When the solubility limit for oxygen is approached during the preoxidation phase (approx. 7 wt.%, corresponding to $x = 0.21$ and DoR = 0.45), the two-phase mixture of oxide and nitride forms easily, as can be seen in Fig. 3. For oxygen contents of less than

4 wt.%, almost no formation of ZrN was observed, although considerable mass gain due to dissolution of nitrogen in the α -Zr phase was seen during the nitriding phase.

Inhomogeneous reactions, as seen in some of the tests, naturally influence the kinetic evaluation of the experiments. Nevertheless, rate constants based on linear reaction kinetics according to Eq. (4) have been determined for all tests.

$$\frac{\Delta m}{S} = K_N \cdot t \quad (4)$$

with Δm denoting mass gain, S denoting sample surface, K_N denoting rate constant, and t denoting time. The rate constants were determined based on the linear fitting of $(\Delta m/S) = f(t)$, neglecting initial effects and deviations from the linear behavior due to approaching saturation. Only the curved surfaces of the tube segment were taken into account for the calculation of the surface, leading to a better approximation for high degrees of reaction.

Fig. 9 summarizes the results of all tests, showing the linear nitriding rate constants in dependence on the initial oxygen content in the metal (A) and on the temperature (B). At least for samples completely in the α -Zr(O,N) phase region, i.e., for $C_0 \geq 3$ wt.%, the temperature dependence follows Arrhenius-type behavior up to 1300°C; this dependence then decreases for all samples (except for $C_0 = 1$ –2 at.%) at 1400°C. The general temperature dependence is analogous to the reaction kinetics between zirconium alloys in air atmosphere, for which a decrease of reaction rate at very high temperatures ($\geq 1400^\circ\text{C}$) was found as well [9]. The reason for this unusual dependence on temperature is not yet clear. Possible explanations could be the formation of one-phase oxynitrides instead of a two-phase mixture oxide/nitride at the highest temperatures, as discussed in study by Lerch et al. [17], or high oxygen diffusion at increased temperatures, leading to an oxide barrier before the nitride can become active.

There is a strong dependence of the reaction kinetics on the oxygen content in the metal, as can be seen in Fig. 6. Several

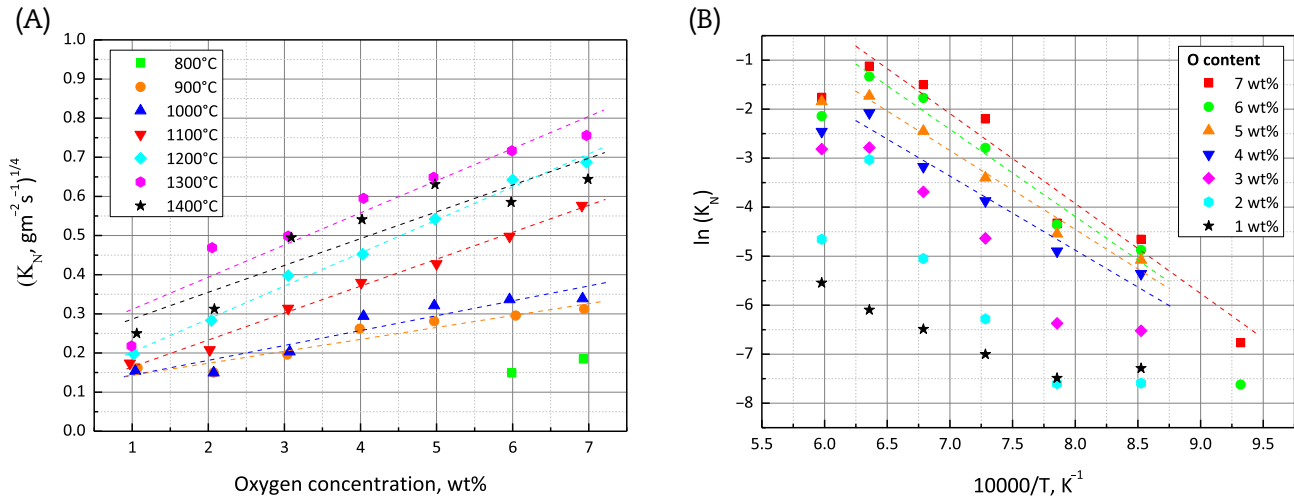


Fig. 9. Linear rate constants of the nitriding of α -Zr(O). (A) In dependence on oxygen content. (B) Temperature (Arrhenius diagram).

attempts at fitting have been made to find correlations in these data. As already observed for Zircaloy-4 [1], the best fits were obtained for the correlation $\sqrt[4]{K_N} = f(C_{oxygen})$, as is illustrated in the Fig. 9A. This very strong dependency may be connected to the low diffusion coefficient of nitrogen in α -Zr, which is two orders of magnitude lower than that of oxygen [18,19]. The lower the oxygen concentration in the bulk materials, the more nitrogen has to be taken up to reach the saturation limit. Another factor is an effect in which the oxygen content increases the lattice parameters [1], which may affect diffusion.

The most relevant results for better understanding and modeling of zirconium oxidation in nitrogen-containing atmospheres are the reaction rates of the oxygen saturated zirconium with nitrogen because this is the phase that is in equilibrium with the oxide at the metal-oxide interface. The corresponding Arrhenius equation, neglecting the data point for 1400°C, is given in Eq. (6).

$$K_N = 1.0 \cdot 10^5 \cdot \exp\left(\frac{-161600}{RT}\right) \quad (\text{for } C_{oxygen} = 7\text{wt.}\%, T = 800 - 1300^\circ\text{C}, p_{N_2} = 0.77\text{bar}) \quad (6)$$

Fig. 10A condenses the reaction rates of all tests performed as a function of temperature and oxygen content into a 3D diagram that clearly reveals the highest reaction rates at 1300°C and the

maximal oxygen content. With respect to the general mechanism and the magnitude of the nitriding rates (Fig. 10B), the data obtained for the Nb-based M5[®] alloy match with the data of a previous study on Zircaloy-4 cladding segments [1]. Interestingly, the maximum nitriding rates for the tin-bearing Zircaloy-4 were measured at 1200°C, i.e., 100 K below the maximum value for M5[®].

It should be mentioned again that the strong influence of the thermal–hydraulic boundary conditions and the stochastic nature of nitrogen attack partly caused locally inhomogeneous reaction behavior. Hence, the overall results may be taken as semi-quantitative. In any case, the most important results obtained with saturated α -Zr(O) phase (7 wt.% oxygen at the metal-oxide interface) are reliable because of the clear linear kinetics up to 1300°C and the very homogeneous reaction behavior compared with that of the samples with lower oxygen preloading. Furthermore, the nitrogen partial pressure was constant (0.77 bar) during all tests, and no statement can be made on the dependence of the reaction rates on the nitrogen partial pressure from the experiments presented here. For a better understanding of the complex behavior of the Zr-O-N system, a thermodynamic analysis of the ternary system is needed, one that includes systematic study of the mutual solubility of nitrogen in Zr-O and oxygen in Zr-N, as well as clarification of whether ternary phases can form under conditions of severe nuclear accidents.

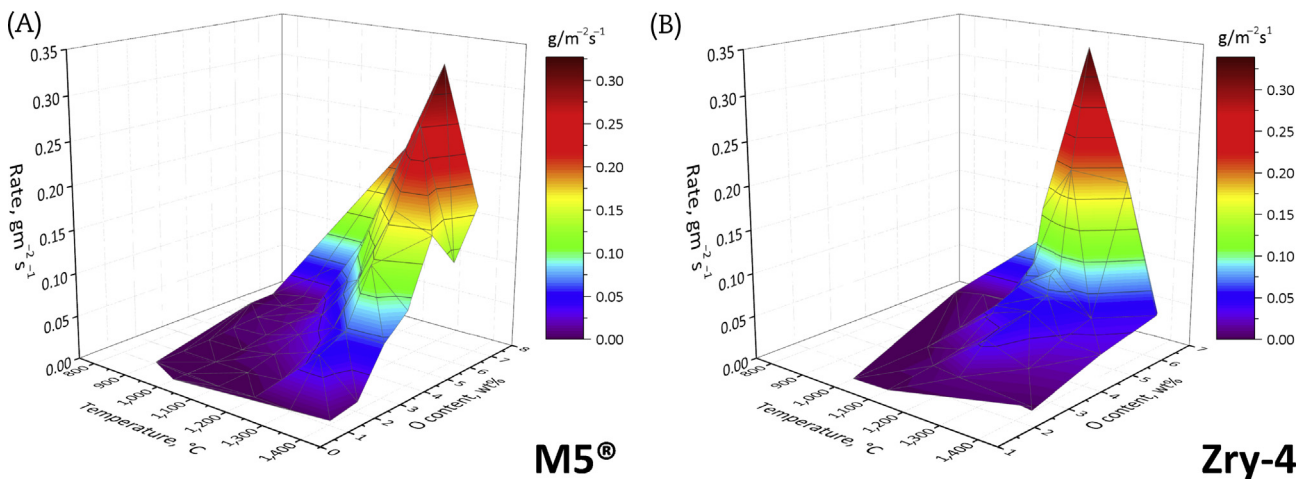


Fig. 10. Linear rate constants of the nitriding of α -Zr(O) in dependence on oxygen content and temperature. (A) For M5[®] (this work). (B) For Zircaloy-4 (data from Ref. [1]).

5. Summary

This article presents results on the reaction between oxygen-stabilized α -Zr(O), prepared from the AREVA alloy M5[®] and nitrogen. A wide range of temperatures (800–1400°C) and compositions of the α -Zr(O) phase (1–7 wt.% oxygen) was investigated in thermogravimetric experiments. This study supplements a previous article on the oxygen-stabilized Zircaloy-4 reaction with nitrogen which for the first time presented data on the reaction kinetics of oxygen stabilized α -Zr(O) with nitrogen [1]. The outcomes of the two studies are quite comparable in terms of the general mechanisms and values of the nitriding rate constants, except for a shift of the maximum nitriding rates by 100 K.

The reaction between oxygen-stabilized zirconium and nitrogen has linear kinetics and is 1–2 orders of magnitude faster than the reaction of the oxygen-free metal with nitrogen. Strong dependences on temperature and on the initial composition of α -Zr(O) were found. The reaction kinetics becomes faster with increasing temperature up to 1300°C; kinetics slows down with further rising of the temperature. The strong dependence on the oxygen content in the metal can be best described using a fourth root correlation of the linear reaction rate constants.

Conflict of interest

The authors declare that there is no conflict of interest.

Acknowledgments

This work was sponsored by the HGF program NUSAFE at Karlsruhe Institute of Technology. The authors would like to thank U. Stegmaier and P. Severloh for their support in the posttest examinations.

References

- [1] M. Steinbrück, High-temperature reaction of oxygen-stabilized α -Zr(O) with nitrogen, *J. Nuclear Mater.* 447 (2014) 46–55.
- [2] M. Steinbrück, M. Große, L. Sepold, J. Stuckert, Synopsis and outcome of the QUENCH experimental program, *Nuclear Eng. Design* 240 (2010) 1714–1727.
- [3] B. Cox, Some thoughts on the mechanisms of in-reactor corrosion of zirconium alloys, *J. Nuclear Mater.* 336 (2005) 331–368.
- [4] G. Schanz, B. Adroguer, A. Volchek, Advanced treatment of zircaloy cladding high-temperature oxidation in severe accident code calculations Part I. Experimental database and basic modeling, *Nuclear Eng. Design* 232 (2004) 75–84.
- [5] D.A. Powers, L.N. Kmetyk, R.C. Schmidt, A Review of Technical Issues of Air Ingression during Severe Reactor Accidents, 1994.
- [6] OECD-NEA/CSNI, Status Report on Spent Fuel Pools Under Loss-of-Cooling and Loss-of-Coolant Accident Conditions, Report NEA/CSNI/R(21015)2, 2015.
- [7] E.T. Hayes, A.H. Roberson, Some effects of heating zirconium in air, oxygen, and nitrogen, *J. Electrochem. Soc.* 96 (1949) 142–151.
- [8] C.J. Rosa, W.W. Smeltzer, The oxidation of zirconium on oxygen-nitrogen atmospheres, *Z. Metallkunde* 71 (1980) 470–475.
- [9] M. Steinbrück, Prototypical experiments relating to air oxidation of Zircaloy-4 at high temperatures, *J. Nuclear Mater.* 392 (2009) 531–544.
- [10] C. Duriez, T. Dupont, B. Schmet, F. Enoch, Zircaloy-4 and M5[®] high temperature oxidation and nitriding in air, *J. Nuclear Mater.* 380 (2008) 30–45.
- [11] M. Steinbrück, M. Böttcher, Air oxidation of Zircaloy-4, M5[®] and ZIRLO[™] cladding alloys at high temperatures, *J. Nuclear Mater.* 414 (2011) 276–285.
- [12] M. Steinbrück, M. Grosse, Deviations from Parabolic Kinetics during Oxidation of Zirconium Alloys, vol. STP 1543, ASTM Special Technical Publication, 2015, pp. 979–1001.
- [13] M. Steinbrück, S. Schaffer, High-temperature oxidation of Zircaloy-4 in oxygen–nitrogen mixtures, *Oxid. Metals* 85 (2016) 245–262.
- [14] M. Steinbrück, U. Stegmaier, T. Ziegler, Prototypical Experiments on Air Oxidation of Zircaloy-4 at High Temperatures, Forschungszentrum Karlsruhe, Report FZKA 7257, 2007.
- [15] P. Hofmann, S. Hagen, S. Schanz, A. Skokan, Chemical Interactions of Reactor Core Materials Up to Very High Temperatures, Kernforschungszentrum Karlsruhe, Report KFK-4485, 1989.
- [16] M. Steinbrück, Hydrogen absorption by zirconium alloys at high temperatures, *J. Nuclear Mater.* 334 (2004) 58–64.
- [17] M. Lerch, et al., Oxide nitrides: from oxides to solids with mobile nitrogen ions, *Prog. Solid State Chem.* 37 (2009) 81–131.
- [18] A. Anttila, J. Räisänen, J. Keinonen, Diffusion of nitrogen in α -Zr AND α -Hf, *J. Less Common Metals* 96 (1984) 257–262.
- [19] I.G. Ritchie, A. Atrens, The diffusion of oxygen in alpha-zirconium, *J. Nuclear Mater.* 67 (1977) 254–264.